Tang *et al.*
Chinese Journal of Mechanical Engineering (2023) 36:49
https://doi.org/10.1186/s10033-023-00866-w

Chinese Journal of Mechanical Engineering

ORIGINAL ARTICLE

Open Access

Influence of Non-uniform Parameter of Bolt Joint on Complexity of Frequency Characteristics of Cylindrical Shell

Qiansheng Tang[1,2], Houxin She[2], Chaofeng Li[2,3*] and Bangchun Wen[2]

Abstract

Bolt connection is one of the main fixing methods of cylindrical shell structures. A typical bolted connection model is considered as a tuned system. However, in the actual working conditions, due to the manufacturing error, installation error and uneven materials of bolts, there are always random errors between different bolts. To investigate the influence of non-uniform parameters of bolt joint, including the stiffness and the distribution position, on frequency complexity characteristics of cylindrical shell through a statistical method is the main aim of this paper. The bolted joints considered here were simplified as a series of springs with random features. The vibration equation of the bolted joined cylindrical shell was derived based on Sanders' thin shell theory. The Monte Carlo simulation and statistical theory were applied to the statistical analysis of mode characteristics of the system. First, the frequency and mode shape of the tuned system were investigated and compared with FEM. Then, the effect of the random distribution and the random constraint stiffness of the bolts on the frequency and mode shape were studied. And the statistical analysis on the natural frequencies was evaluated for different mistuned levels. And some special cases were presented to help understand the effect of random mistuning. This research introduces random theory into the modeling of bolted joints and proposes a reference result to interpret the complexity of the modal characteristics of cylindrical shells with non-uniform parameters of bolt joints.

Keywords Bolted joint, Random mistuning, Shell vibration, Mode shape, Statistical analysis

1 Introduction

The structure of the cylindrical shell is usually utilized in a lot of mechanical systems such as aerospace, submarines, due to its relatively small weight and load carrying capacity. However, there are some inherent variations in the structure, especially in the geometric parameter and the restraint condition of the cylindrical shell. Therefore, the random vibration of the cylindrical shell has been also a hot topic for researchers. The random problem of the cylindrical shell has been reported mainly about the material and geometric imperfection or random excitations.

Material and geometric imperfection is an important source which cause the random shell vibration. For example, taking random scatter in the material properties into account, Yadav et al. [1, 2] developed a unified approach to solve vibration problem of composite cylindrical shells, and some specific problems were simulated. Rodrigues [3, 4] studied the nonlinear response of cylindrical shells with geometric imperfections. Random excitation is another important source which cause the random vibration of the structure such as beam [5], plate [6] and shell [7]. For example, Dogan et al. [7] reported

*Correspondence:
Chaofeng Li
chfli@mail.neu.edu.cn
[1] School of Engineering, Anhui Agricultural University, Hefei 230036, China
[2] School of Mechanical Engineering and Automation, Northeastern University, Shenyang 110819, China
[3] Key Laboratory of Vibration and Control of Aero-Propulsion System, Ministry of Education, Northeastern University, Shenyang 110819, China

nonlinear flexural vibration of cylindrical shell under random pressure, random point loads or thermal effects.

However, up to now, there are few open articles found about the vibration of a single cylindrical shell considering the random problem about the bolted joints. Arbitrary and point support boundary condition was considered into the cylindrical shell to study uniformly and the non-uniformly supported cylindrical shell by Dai et al. [8], Qin et al. [9], Zhou et al. [10], Chen et al. [11], Xie et al. [12] and Li et al. [13]. For bolted joined cylindrical shell structure, some literatures have been reported. Li et al. [14] studied the mode frequency and shape of the thin cylindrical shell under bolt looseness boundary through the FE method and experimental test method. Qin et al. [15] studied the influence of bolt loosening on the vibration of disk-drum rotor by nonlinear FE simulations and harmonic balance method. The restraint condition on the cylindrical shell structure varies with the change of the bolted joint about the preload, excitation, distribution, and so on. Liao et al. [16, 17] established a general dynamic model of bolted lap structure and a dynamic model of bolted lap structure with viscoelastic layer, and analyzed the influence of Coulomb friction and excitation level on the harmonic response of the system. Zhu et al. [18, 19] put forward an analytical model for evaluating the elastic interaction of bolt flange contact caused by the tightening process, and an analytical model for the change of bolt tensile load caused by the elastic combination interaction. Farhad et al. [20] used the combination of linear translational spring, linear and nonlinear torsional spring and linear torsional damper to establish the model of bolt overlap interface, and used harmonic balance method and numerical simulation to analytically solve the coupled nonlinear equations. Armand et al. [21] analyzed the influence of surface roughness on the contact pressure distribution, local contact stiffness and nonlinear dynamic response of bolted connections using multi-scale method. Li et al. [22] studied the nonlinear vibration of fiber reinforced composite cylindrical shells with bolted boundary conditions from both theoretical and experimental aspects, taking into account the material characteristics related to the nonlinear amplitude of fiber reinforced composite materials and the boundary conditions of partial loosening of bolts. Refs. [23, 24] proposed a semi analytical modeling method for bolted thin-walled cylindrical shells, and further analyzed their vibration response and interface contact state. The vibration characteristics of bolted cylindrical shells are studied. Li et al. [25] studied the free vibration and forced vibration of the cylinder cylinder composite shell with partially bolted loose connections from both experimental and theoretical aspects. Yang et al. [26] established the finite element model of the bolted rotating flexible shaft disk drum system based on the beam shell spring mixed element and the self-developed finite element program. The rotation effects, such as centrifugal effect, initial tension, gyro moment and geometric nonlinearity caused by large deformation, are considered. Pirdayr et al. [27] studied the vibration characteristics of six bolt connecting plates by using test and finite element methods. Consider the influence of bolt looseness on vibration characteristics. Du et al. [28] proposed a unified discontinuous variable stiffness model to simulate the actual connection of bolts by improving the artificial spring technology, which is used to analyze the dynamics of rotating cylindrical shells.

Bolted joint is a common restraint method for shell structure, and it determines the boundary condition of the cylindrical shell. In fact, there are also many uncertainties and random characteristics appearing at the bolted joint, which leads to non-uniform parameters of bolt joints. These problems may be caused by the following source. Firstly, due to manufacturing errors, the contact surfaces of the bolted joint hardly keep consistent. Secondly, the distribution of the bolts is not absolutely symmetric. Thirdly, the initial preload of the bolts affect the connection effect [29]. Fourthly, the external excitation leads to the non-linear characteristic of the bolted joint [30]. Fifthly, bolt loosening can also cause the variation of the restraint stiffness [14]. And there are also lots of many other sources for the uncertainty characteristics of bolted joints [31], including random bolt distribution and random restraint stiffness distribution. The unsymmetrical bolt distribution and stiffness distribution are defined as the mistuning patterns studied in this paper.

Therefore, in this paper, the random theory is considered into the modeling of bolted joints and the main issue is to investigate the effect of random mistuning bolted joints, including the bolt distribution mistuning and the restraint stiffness mistuning, on the mode characteristics of the cylindrical shell. The dynamic model of a single cylindrical shell with bolted joints was established and the statistical analysis was done utilizing the Monte Carlo simulation method. The frequency's means

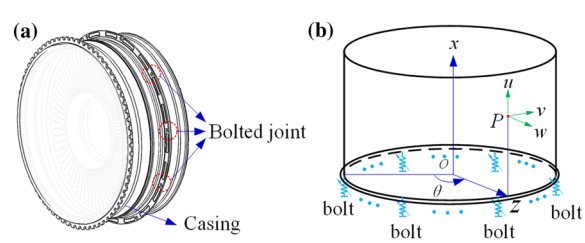

Figure 1 Sketch of cylindrical shell with bolted joints and coordinate establishment

and probability density, and confidence interval of the frequency mean were investigated in the numerical simulation.

2 Mathematical Formulation

In aerospace, the aero-engine casings are consist of many thin-walled shell structures, some of which are assembled by bolted joints, for example, shown in Figure 1a. And Figure 1b present the sketch of a cylindrical shell and a coordinate system, which can clearly express the motion of the shell wall. The motion of a certain point P is expressed as u, v, and w, respectively. The bolts are represented by a series of springs.

The strain expression of the cylindrical shell, according to Sanders' shell theory, can be expressed as:

$$\begin{aligned} \varepsilon_x^0 &= \frac{\partial u}{\partial x}, \\ \varepsilon_\theta^0 &= \frac{\partial v}{R\partial\theta} + \frac{w}{R}, \\ \varepsilon_{x\theta}^0 &= \frac{\partial u}{R\partial\theta} + \frac{\partial v}{\partial x}, \end{aligned} \tag{1}$$

$$\begin{aligned} \chi_x &= -\frac{\partial^2 w}{\partial x^2}, \\ \chi_\theta &= \frac{\partial v}{R^2\partial\theta} - \frac{\partial^2 w}{R^2\partial\theta^2}, \\ \chi_{x\theta} &= -\frac{\partial u}{2R^2\partial\theta} + \frac{3\partial v}{2R\partial x} - \frac{2\partial^2 w}{R\partial x\partial\theta}. \end{aligned} \tag{2}$$

The kinetic energy and the strain energy of the bolted joined cylindrical shell can be written by:

$$T = \frac{1}{2}\rho h \int_0^L \int_0^{2\pi} \left[\left(\frac{\partial u}{\partial t}\right)^2 + \left(\frac{\partial v}{\partial t}\right)^2 + \left(\frac{\partial w}{\partial t}\right)^2 \right] R\mathrm{d}x\mathrm{d}\theta, \tag{3}$$

$$\begin{aligned} U_\varepsilon &\int_0^L \int_0^{2\pi} \frac{Eh}{2(1-\mu^2)} \left[\left(\varepsilon_x^0 + \varepsilon_\theta^0\right) - 2(1-\mu)\left(\varepsilon_x^0\varepsilon_\theta^0 - \frac{{\varepsilon_{x\theta}^0}^2}{4}\right)\right] R\mathrm{d}x\mathrm{d}\theta \\ &+ \int_0^L \int_0^{2\pi} \frac{Eh^3}{24(1-\mu^2)} \left[(\chi_x + \chi_\theta)^2 - (1-\mu)\left(\chi_x\chi_\theta - \frac{\chi_{x\theta}^2}{4}\right)\right] R\mathrm{d}x\mathrm{d}\theta. \end{aligned} \tag{4}$$

Therefore, substituting Eqs. (1)–(2) into Eq. (4):

$$\begin{aligned} U_\varepsilon = \int_0^L \int_0^{2\pi} \Bigg\{ &\frac{Eh}{2(1-\mu^2)} \left[\left[\begin{array}{l} \left(\frac{\partial u}{\partial x}\right)^2 + \frac{2\mu}{R}\frac{\partial u}{\partial x}\left(\frac{\partial v}{\partial\theta} + w\right) + \\ \frac{1}{R^2}\left(\frac{\partial v}{\partial\theta} + w\right)^2 + \frac{1-\mu}{2}\left(\frac{1}{R}\frac{\partial u}{\partial\theta} + \frac{\partial v}{\partial x}\right)^2 \end{array} \right] \right. \\ &+ \frac{Eh^3}{24(1-\mu^2)} \left[\begin{array}{l} \left(\frac{\partial^2 w}{\partial x^2}\right)^2 + \frac{2\mu}{R^2}\frac{\partial^2 w}{\partial x^2}\left(\frac{\partial^2 w}{\partial\theta^2} - \frac{\partial v}{\partial\theta}\right) \\ + \frac{1}{R^4}\left(\frac{\partial v}{\partial\theta} - \frac{\partial^2 w}{\partial\theta^2}\right)^2 \\ + \frac{(1-\mu)}{2R^2}\left(\frac{1}{2R}\frac{\partial u}{\partial\theta} - \frac{3}{2}\frac{\partial v}{\partial x} + \frac{2\partial^2 w}{\partial x\partial\theta}\right)^2 \end{array} \right] \Bigg\} R\mathrm{d}x\mathrm{d}\theta. \end{aligned} \tag{5}$$

For a shell, defining $\xi = x/L$, the displacements can be assumed as:

$$\begin{aligned} u(\xi,\theta,t) &= \sum_{n=0}^{N_n}\sum_{m=1}^{NT} \begin{matrix} p_{mn}^{c}(t)\varphi_m^{u}(\xi)\cos(n\theta) \\ +p_{mn}^{s}(t)\varphi_m^{u}(\xi)sin(n\theta) \end{matrix} \\ &= \boldsymbol{U}^{\mathrm{T}}(\xi,\theta)\boldsymbol{p}(t), \\ v(\xi,\theta,t) &= \sum_{n=0}^{N_n}\sum_{m=1}^{NT} \begin{matrix} q_{mn}^{s}(t)\varphi_m^{v}(\xi)\sin(n\theta) \\ +q_{mn}^{c}(t)\varphi_m^{v}(\xi)\cos(n\theta) \end{matrix} \\ &= \boldsymbol{V}^{\mathrm{T}}(\xi,\theta)\boldsymbol{q}(t), \\ w(\xi,\theta,t) &= \sum_{n=0}^{N_n}\sum_{m=1}^{NT} \begin{matrix} r_{mn}^{c}(t)\varphi_m^{w}(\xi)\cos(n\theta) \\ +r_{mn}^{s}(t)\varphi_m^{w}(\xi)\sin(n\theta) \end{matrix} \\ &= \boldsymbol{W}^{\mathrm{T}}(\xi,\theta)\boldsymbol{r}(t), \end{aligned} \tag{6}$$

where $\boldsymbol{U}$, $\boldsymbol{V}$, $\boldsymbol{W}$ are the vectors, whose elements are the functions about ξ and θ. $\varphi_m^u(\xi)$, $\varphi_m^v(\xi)$ and $\varphi_m^w(\xi)$ are the characteristic orthogonal polynomials [12]. $\boldsymbol{p}$, $\boldsymbol{q}$, $\boldsymbol{r}$ are the vectors, whose elements are the functions about time. p_{mn}^c, q_{mn}^c, r_{mn}^c, p_{mn}^s, q_{mn}^s, r_{mn}^s are the parameters about time.

For bolted joint, the restraint on the boundary of the cylindrical shell is always discrete, which causes the characteristics of the large local restraint. To discuss the local restraint, the bolted joint will be simplified to be linear point restraints to study its natural characteristics (frequency and mode shape). The restraint model of the bolt is theoretically established in four directions about the axial, circumferential, radial and rotational directions. The bolt can be numbered as S ($S = 1, 2, 3, \ldots, N_b$). The positions of the bolt in the coordinate system are assumed as θ_S. The energy stored in the bolted joints will be expressed:

$$U_{\mathrm{bolt}} = \sum_{S=1}^{N_b}\left(\frac{1}{2}k_{\theta_S}^{u}u_{\theta_S}^2 + \frac{1}{2}k_{\theta_S}^{v}v_{\theta_S}^2 + \frac{1}{2}k_{\theta_S}^{w}w_{\theta_S}^2 + \frac{1}{2}k_{\theta_S}^{\theta}\left(\frac{\partial w_{\theta_S}}{\partial x}\right)^2\right). \tag{7}$$

Substituting Eq. (6) into Eqs. (3), (5), (7), the discretized kinetic and potential energy can be got. Then, Substituting them into Lagrange equation, the free vibration equation of the structure can be obtained:

$$\boldsymbol{M}\ddot{\boldsymbol{X}} + \boldsymbol{K}\boldsymbol{X} = \boldsymbol{0}, \tag{8}$$

where

$$\boldsymbol{M} = \begin{bmatrix} \boldsymbol{M}_1 & & \\ & \boldsymbol{M}_2 & \\ & & \boldsymbol{M}_3 \end{bmatrix}, \boldsymbol{X} = \begin{bmatrix} \boldsymbol{p} \\ \boldsymbol{q} \\ \boldsymbol{r} \end{bmatrix},$$

$$\boldsymbol{K} = \begin{bmatrix} \boldsymbol{K}_1 + \boldsymbol{B}_2 & \frac{1}{2}\boldsymbol{K}_2 & \frac{1}{2}\boldsymbol{K}_3 \\ \frac{1}{2}\boldsymbol{K}_2 & \boldsymbol{K}_4 + \boldsymbol{B}_2 & \frac{1}{2}\boldsymbol{K}_5 \\ \frac{1}{2}\boldsymbol{K}_3^{\mathrm{T}} & \frac{1}{2}\boldsymbol{K}_5^{\mathrm{T}} & \boldsymbol{K}_6 + \boldsymbol{B}_3 \end{bmatrix}.$$

The detailed expressions of the matrixes are listed as follows:

$$\boldsymbol{M}_1 = \rho hL\int_0^1\int_0^{2\pi}\boldsymbol{U}\boldsymbol{U}^{\mathrm{T}}R\mathrm{d}\theta\mathrm{d}\xi,$$

$$\boldsymbol{M}_2 = \rho hL\int_0^1\int_0^{2\pi}\boldsymbol{V}\boldsymbol{V}^{\mathrm{T}}R\mathrm{d}\theta\mathrm{d}\xi,$$

$$\boldsymbol{M}_3 = \rho hL\int_0^1\int_0^{2\pi}\boldsymbol{W}\boldsymbol{W}^{\mathrm{T}}R\mathrm{d}\theta\mathrm{d}\xi,$$

$$\boldsymbol{K}_1 = \int_0^1\int_0^{2\pi}\left\{\begin{matrix} \frac{Eh}{(1-\mu^2)}\frac{1}{L^2}\frac{\partial\boldsymbol{U}}{\partial\xi}\frac{\partial\boldsymbol{U}^{\mathrm{T}}}{\partial\xi} + \\ \left[\frac{Eh}{(1-\mu^2)}\frac{1-\mu}{2}\frac{1}{R^2} + \right. \\ \left.\frac{Eh^3}{12(1-\mu^2)}\frac{(1-\mu)}{2R^2}\frac{1}{4R^2}\right]\frac{\partial\boldsymbol{U}}{\partial\theta}\frac{\partial\boldsymbol{U}^{\mathrm{T}}}{\partial\theta} \end{matrix}\right\}RL\mathrm{d}\theta\mathrm{d}\xi,$$

$$\boldsymbol{K}_2 = \int_0^1\int_0^{2\pi}\left\{\begin{matrix} \frac{Eh}{(1-\mu^2)}\frac{2\mu}{RL}\frac{\partial\boldsymbol{U}}{\partial\xi}\frac{\partial\boldsymbol{V}^{\mathrm{T}}}{\partial\theta} + \\ \left[\frac{Eh}{(1-\mu^2)}\frac{1-\mu}{2}\frac{2}{RL} - \right. \\ \left.\frac{Eh^3}{12(1-\mu^2)}\frac{(1-\mu)}{2R^2}\frac{3}{2RL}\right]\frac{\partial\boldsymbol{U}}{\partial\theta}\frac{\partial\boldsymbol{V}^{\mathrm{T}}}{\partial\xi} \end{matrix}\right\}RL\mathrm{d}\theta\mathrm{d}\xi,$$

$$\boldsymbol{K}_3 = \int_0^1\int_0^{2\pi}\left\{\begin{matrix} \frac{Eh}{(1-\mu^2)}\frac{2\mu}{RL}\frac{\partial\boldsymbol{U}}{\partial\xi}\boldsymbol{W}^{\mathrm{T}} + \\ \frac{Eh^3}{12(1-\mu^2)}\frac{(1-\mu)}{2R^2}\frac{2}{RL}\frac{\partial\boldsymbol{U}}{\partial\theta}\frac{\partial^2\boldsymbol{W}^{\mathrm{T}}}{\partial\xi\partial\theta} \end{matrix}\right\}RL\mathrm{d}\theta\mathrm{d}\xi,$$

$$\boldsymbol{K}_4=\int_0^1\int_0^{2\pi}\left\{\begin{array}{l}\left[\dfrac{Eh}{(1-\mu^2)}\dfrac{1}{R^2}+\right.\\ \left.\dfrac{Eh^3}{12(1-\mu^2)}\dfrac{1}{R^4}\right]\dfrac{\partial\boldsymbol{V}}{\partial\theta}\dfrac{\partial\boldsymbol{V}^{\mathrm{T}}}{\partial\theta}+\\ \left[\dfrac{Eh}{(1-\mu^2)}\dfrac{1-\mu}{2}\dfrac{1}{L^2}+\right.\\ \left.\dfrac{Eh^3}{12(1-\mu^2)}\dfrac{(1-\mu)}{2R^2}\dfrac{9}{4L^2}\right]\dfrac{\partial\boldsymbol{V}}{\partial\xi}\dfrac{\partial\boldsymbol{V}^{\mathrm{T}}}{\partial\xi}\end{array}\right\}RL\mathrm{d}\theta\mathrm{d}\xi,$$

$$\boldsymbol{K}_5=\int_0^1\int_0^{2\pi}\left\{\begin{array}{l}\dfrac{Eh}{(1-\mu^2)}\dfrac{2}{R^2}\dfrac{\partial\boldsymbol{V}}{\partial\theta}\boldsymbol{W}^{\mathrm{T}}-\\ \dfrac{Eh^3}{12(1-\mu^2)}\dfrac{2\mu}{R^2L^2}\dfrac{\partial\boldsymbol{V}}{\partial\theta}\dfrac{\partial^2\boldsymbol{W}^{\mathrm{T}}}{\partial\xi^2}-\\ \dfrac{Eh^3}{12(1-\mu^2)}\dfrac{2}{R^4}\dfrac{\partial\boldsymbol{V}}{\partial\theta}\dfrac{\partial^2\boldsymbol{W}^{\mathrm{T}}}{\partial\theta^2}-\\ \dfrac{Eh^3}{12(1-\mu^2)}\dfrac{(1-\mu)}{2R^2}\dfrac{6}{L^2}\dfrac{\partial\boldsymbol{V}}{\partial\xi}\dfrac{\partial^2\boldsymbol{W}^{\mathrm{T}}}{\partial\xi\partial\theta}\end{array}\right\}RL\mathrm{d}\theta\mathrm{d}\xi,$$

$$\boldsymbol{K}_6=\int_0^1\int_0^{2\pi}\left\{\begin{array}{l}\dfrac{Eh}{(1-\mu^2)}\dfrac{1}{R^2}\boldsymbol{W}\boldsymbol{W}^{\mathrm{T}}+\\ \dfrac{Eh^3}{12(1-\mu^2)}\dfrac{1}{L^4}\dfrac{\partial^2\boldsymbol{W}}{\partial\xi^2}\dfrac{\partial^2\boldsymbol{W}^{\mathrm{T}}}{\partial\xi^2}+\\ \dfrac{Eh^3}{12(1-\mu^2)}\dfrac{2\mu}{R^2L^2}\dfrac{\partial^2\boldsymbol{W}}{\partial\xi^2}\dfrac{\partial^2\boldsymbol{W}^{\mathrm{T}}}{\partial\theta^2}+\\ \dfrac{Eh^3}{12(1-\mu^2)}\dfrac{1}{R^4}\dfrac{\partial^2\boldsymbol{W}}{\partial\theta^2}\dfrac{\partial^2\boldsymbol{W}^{\mathrm{T}}}{\partial\theta^2}+\\ \dfrac{Eh^3}{12(1-\mu^2)}\dfrac{(1-\mu)}{2R^2}\dfrac{4}{L^2}\dfrac{\partial^2\boldsymbol{W}}{\partial\xi\partial\theta}\dfrac{\partial^2\boldsymbol{W}^{\mathrm{T}}}{\partial\xi\partial\theta}\end{array}\right\}RL\mathrm{d}\theta\mathrm{d}\xi,$$

$$\boldsymbol{B}_1=\sum_{S=1}^{N_b}k_{\theta_S}^{u}\boldsymbol{U}\boldsymbol{U}^{\mathrm{T}}\Big|_{\xi=0,\theta=\theta_S},\ \boldsymbol{B}_2=\sum_{S=1}^{N_b}k_{\theta_S}^{v}\boldsymbol{V}\boldsymbol{V}^{\mathrm{T}}\Big|_{\xi=0,\theta=\theta_S},$$

$$\boldsymbol{B}_3=\sum_{S=1}^{N_b}k_{\theta_S}^{w}\boldsymbol{W}\boldsymbol{W}^{\mathrm{T}}\Big|_{\xi=0,\theta=\theta_S}+\sum_{S=1}^{N_b}k_{\theta_S}^{\theta}\left(\frac{\partial\boldsymbol{W}}{L\partial\xi}\right)^2\Bigg|_{\xi=0,\theta=\theta_S}.$$

3 Random Problem and Statistical Law

For the cylindrical shell structure with bolted joints, random mistuning always exists among the bolts due to the manufacturing tolerance, installation error and material irregularity of the bolts and other conditions. Therefore,

Table 1 The geometric and material properties of the cylindrical shell

Parameter	Value
Length L (mm)	100
Thickness h (mm)	2
Radius R (mm)	200
Poisson ratio μ	0.3
Young's modulus E (GPa)	206
Density ρ (kg/m^3)	7850

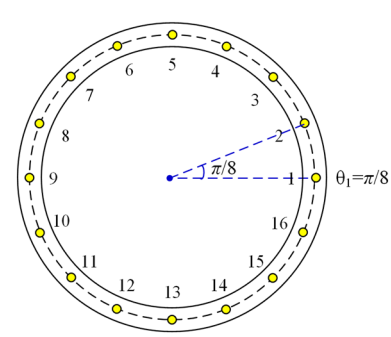

Figure 2 Bolt distribution in the tuned system

some random mistuning parameter is considered into the dynamic model through a random pattern of discrepancies of the relative parameters of the bolts in this paper. The procedure for the random mistuned problem of the bolts, the Monte Carlo simulation method (MCS) can be applied through four steps.

Step 1: N_S samples of mistuned bolt parameters are randomly generated by direct MCS technique. In this paper, two random parameters are introduced and they are the position of the bolts and the restraint stiffness. Therefore, assuming the mistuned error of these two parameters, ρ_θ for the position of the bolts and ρ_k the restraint stiffness of the bolts, to be the normal distribution as

$$\rho_\theta = \frac{(\theta_\mathrm{m} - \theta_\mathrm{t})}{2\pi/N_b} \sim N\left(\mu_\theta, \sigma_\theta^2\right), \tag{9}$$

$$\rho_k = \frac{(k_\mathrm{m} - k_\mathrm{t})}{k_\mathrm{t}} \sim N\left(\mu_k, \sigma_k^2\right), \tag{10}$$

where μ_θ and σ_θ are the mean and standard deviation for the error of the position of bolts, respectively. μ_k and σ_k are the mean and standard deviation for the error of the restraint stiffness of bolts, respectively. θ_t and k_t are the position and the stiffness value of the tuned system. θ_m and k_m is the random position and the random stiffness, generated for the mistuned system.

Step 2: Evaluate the eigenvalues and eigenvectors of the cylindrical shell for each random pattern. From Eq. (8), frequency equation of the system can be obtained:

$$\left|-\omega^2 \boldsymbol{M} + \boldsymbol{K}\right| = \boldsymbol{0}, \tag{11}$$

where ω is the circle frequency of the system and from which the eigenvalues and eigenvectors can be obtained. Therefore, calculations can be done for all the random samples.

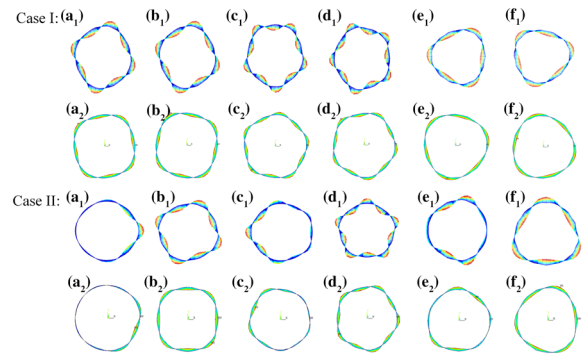

Figure 3 Comparison of mode shapes of the cylindrical shell with tuned bolted joints for Case I and Case II: **a** The first order; **b** the second order; **c** the third order; **d** the forth order; **e** the fifth order; **f** the sixth order (subscript 1 represents the results by the presented method, subscript 2 represents the results by ANSYS)

Step 3: Generate the statistics of mode frequency of the cylindrical shell according to the samples. The MCS method is used to evaluate the probabilistic mode characteristics for all the sample. The mean and standard deviation of the statistical parameter can be obtained:

$$\overline{\omega} = \frac{1}{N} \sum_{i=1}^{N} \left(\omega_i / \omega_\mathrm{t}\right), \tag{12}$$

$$S_\sigma = \sqrt{\frac{\sum_{i=1}^{N} \left(\omega_i / \omega_\mathrm{t} - \overline{\omega}\right)^2}{N_S - 1}}. \tag{13}$$

Step 4: Estimate the confidence for reliability analysis. The confidence interval is performed to quantify the convergence properties of the MCS methods by using student t distribution. A $100(1-\alpha)\%$ confidence interval implies the probability that the frequency of a true sample will fall within the range $\frac{2S_\sigma}{\sqrt{N_S}} t_{\alpha/2}(N_S - 1)$ wide from the estimated values will be $100(1-\alpha)\%$.

$$P\left(\overline{\omega} - \frac{S_\sigma}{\sqrt{N_S}} t_{\alpha/2}(N_S - 1) < \omega < \overline{\omega} + \frac{S_\sigma}{\sqrt{N_S}} t_{\alpha/2}(N_S - 1)\right) = 1 - \alpha, \tag{14}$$

Table 2 Natural frequencies of cylindrical shell with tuned bolted joints (Hz)

	Order	1	2	3	4	5	6
Case I	ω from Eq. (11)	404	404	438	438	488	488
	ω from ANSYS	401	401	438	438	480	480
	Diff. (%)	0.7	0.7	0	0	1.7	1.7
Case II	ω from Eq. (11)	349	404	427	438	462	486
	ω from ANSYS	347	401	426	438	457	477
	Diff. (%)	0.6	0.7	0.2	0	1.1	1.9

where $t_{\alpha/2}$ is the t-value with $N_S - 1$ degrees of freedom in the student t distribution and it is determined by the sample size and the required confidence level due to the unknown variance [32].

4 Model Verification

Before analyzing the vibration of single cylindrical shell with random mistuning bolted joints, the first step is to verify the present model. Here, the natural characteristics of the cylindrical shell with bolted joints are presented and the obtained results will be compared with the results from ANSYS. The values of the relative parameters of the structure are listed in Table 1.

Normally, according to the restraint condition, the cylindrical shell was considered as a tuned case, which here means that the bolts have a homogeneous distribution around the circle of the shell end and the constraint condition at each bolt is the same as others. Here, the mode frequency and shape of the tuned case are investigated to provide a reference for the study on the mistuned cases in the following section. And the case with 16 bolts was discussed in this paper. As shown in Figure 2, the bolts are numbered as 1, 2, 3, ..., S, ..., 16. And the positions are assumed as θ_1, θ_2,

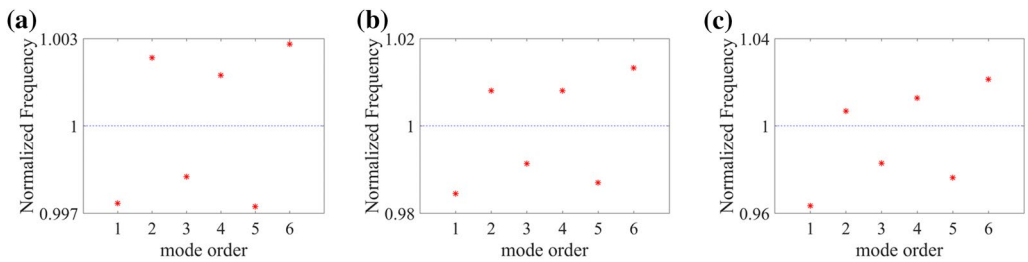

Figure 4 Means of the first six normalized frequencies for mistuned bolt distribution: **a** $\sigma_\theta = 1\%$; **b** $\sigma_\theta = 5\%$; **c** $\sigma_\theta = 10\%$

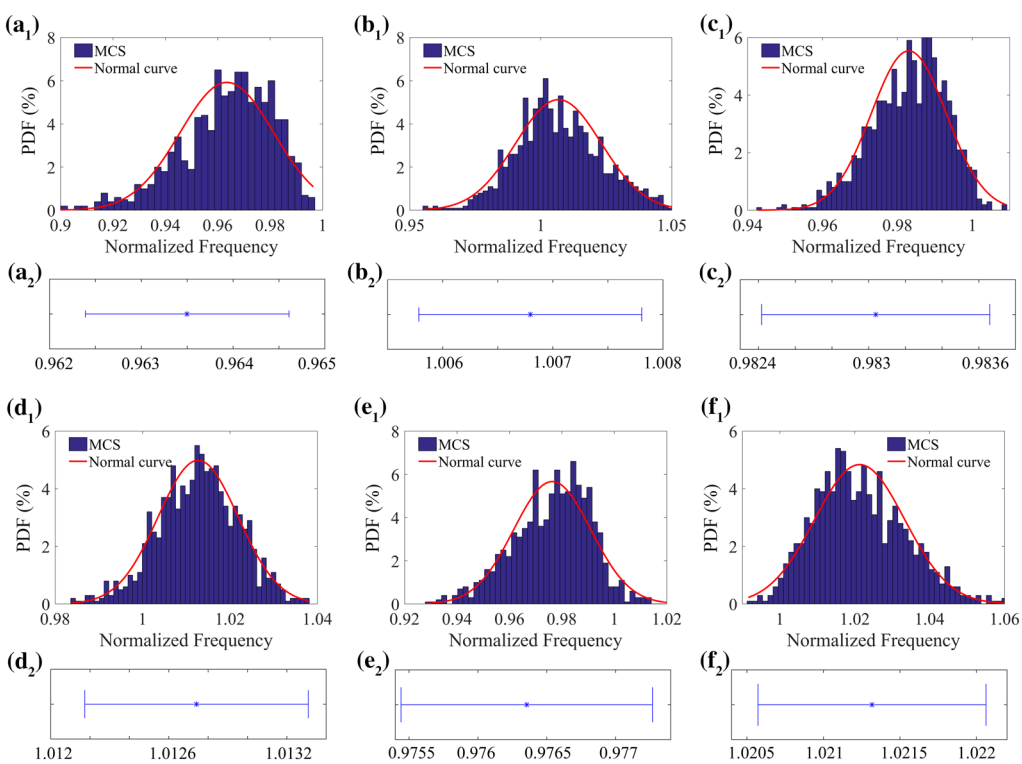

Figure 5 Probability density and the 95% confidence interval and mean of the first six frequencies for 1000 random samples about mistuned bolt distribution: **a** The first order; **b** the second order; **c** the third order; **d** the fourth order; **e** the fifth order; **f** the sixth order (subscript 1 represents the probability density, subscript 2 represents the 95% confidence interval and mean)

Table 3 A random mistuned bolt distribution with the standard deviation $\sigma_\theta = 10\%$

No.	Position	No.	Position
1	0.41381322	9	3.67481505
2	0.85741465	10	4.03574635
3	1.08939253	11	4.26667996
4	1.60465379	12	4.83157014
5	1.97601329	13	5.13357461
6	2.30484169	14	5.49531098
7	2.73186645	15	5.91855411
8	3.15504748	16	6.27513630

θ_3, ..., θ_S, ...θ_{16}, and $\theta_1 = \pi/8$ here. The radian distance between two adjacent bolts is π/8. These means that all the position values can be deduced by a known position of any bolt due to the cyclic symmetry structure of the system. What's more, the restraint stiffness at the position of bolts can be set by the stiffness value. In present case, the stiffness are set to $k^u_{\theta_S}$=1 × 10^7N/m, $k^v_{\theta_S}$=1 × 10^7N/m, $k^w_{\theta_S}$=1 × 10^7N/m, $k^\theta_{\theta_S}$=1 × 10^7N/rad. Two cases are present here as follows: Case I for the tuned bolted joints and Case II for the mistuned bolted joints, in which the No. 16 bolt is missing. Table 2 list the first six natural frequency of cylindrical shell for the two cases. It is obvious that repeated frequencies exist, such as the 1st and 2nd order, with tuned bolted joints. As for Case II, the repeated frequencies bifurcate to two value, which will be investigated in Section 5.3. Figure 3 shows the first six order mode shapes. As shown for Case I, the repeated frequencies have the same mode shapes, and the mode shapes show their symmetry. For Case II, the mode shape shown different shapes, especially for the 1st, 3st and 5nd. At the same time, the finite element model is established by using SHELL 63. COMBINE 14 is selected to simulate the restraint condition. The frequencies and the mode shapes obtained by ANSYS are list in Table 2 and displayed in Figure 3, respectively. By comparing the present results with ANSYS, the difference is very small and a good agreement is shown. And the similar agreement can also be found from the mode shapes. These means the present model is feasible and accurate.

5 Simulation and Discussion

From the forward description, the different position values and stiffness values of the bolted joint can be set to describe the different restraint condition. And the random mistuning case with the non-uniform parameter of bolt joint can also be obtained in this way. In this section, the effects of the bolt distribution random mistuning and the restraint stiffness random mistuning will be studied.

5.1 Effect of the Bolt Distribution Random Mistuning

For bolt joints, their cyclic uniform distribution is the theoretical condition for the bolted joined cylindrical shell. However, due to the manufacturing tolerance or installation error, the position of the bolts may deviate from the optimum location. These phenomena here were called as bolt distribution mistuning. In this section, the case of all the bolts randomly mistuned is discussed. From the investigation above, the case of 16 bolts will be selected as the reference for the analysis of the effect of the bolt distribution mistuning on the vibration characteristics of the cylindrical shell.

For analysis on the random mistuning feature for the position of all the bolts considered into the bolted joined cylindrical shell, the Monte Carlo simulation technique (called MCS for short in the following) is employed. It is assumed the sample number is $N_S = 1000$ and the position error of the bolts follows a normal distribution law N (0, σ_θ^2). What should be pointed out is that

Table 4 The normalized frequencies of cylindrical shell with a random mistuned bolt distribution sample with $\sigma_\theta = 10\%$

Order	1	2	3	4	5	6
Frequency	383.56	404.60	416.96	443.61	451.56	519.60

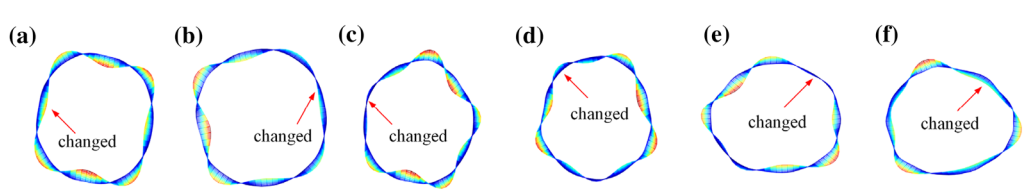

Figure 6 Mode shapes of cylindrical shell for a random mistuned bolt distribution sample with $\sigma_\theta = 10\%$: **a** The first order; **b** the second order; **c** the third order; **d** the fourth order; **e** the fifth order; **f** the sixth order

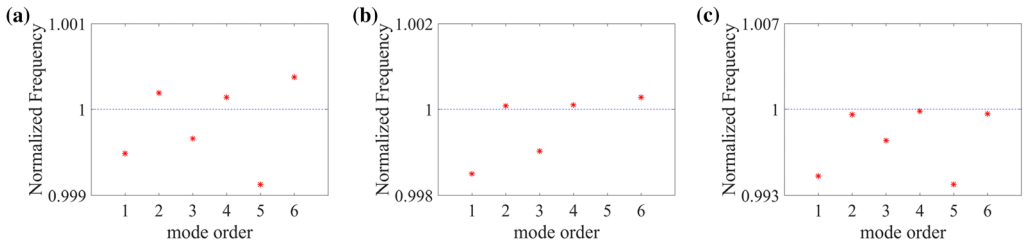

Figure 7 Means of the first six frequency for mistuned restraint stiffness: **a** $\sigma_k = 10\%$; **b** $\sigma_k = 20\%$; **c** $\sigma_k = 30\%$

the normalized frequency used in the following works is defined as the ratio between the natural frequencies of the cylindrical shell with the random mistuned parameters and those of the tuned cases introduced in Section 4. To study the effect of the bolt distribution random mistuning on the cylindrical shell's vibration characteristics, the mean value, confidence interval of means and probability density of the frequencies of the random mistuning cases are investigated under the different standard deviations. In the analysis process in this and the following section, the normalized frequency means the frequency of the tuned system is expressed as the value 1. The minimum and maximum value of the frequency in the samples were assumed as $\omega_{\min}$ and $\omega_{\max}$.

Figure 4 plots the means of the first six frequencies of the cylindrical shell with standard deviations $\sigma_\theta = 1\%$, $\sigma_\theta = 5\%$, and $\sigma_\theta = 10\%$. As shown, the first, third and fifth order normalized frequencies are smaller than 1 and the second, fourth and sixth order normalized frequencies are larger than 1. All the frequency means show the obvious difference from those of the tuning system. The statistics results indicate the random bolt distribution plays a significant role on the cylindrical shell's frequencies. More, as the standard deviation increase, all the normalized frequency are away from 1, and the difference becomes obvious.

The probability density function (called PDF for short in the following), the 95% Confidence interval and mean

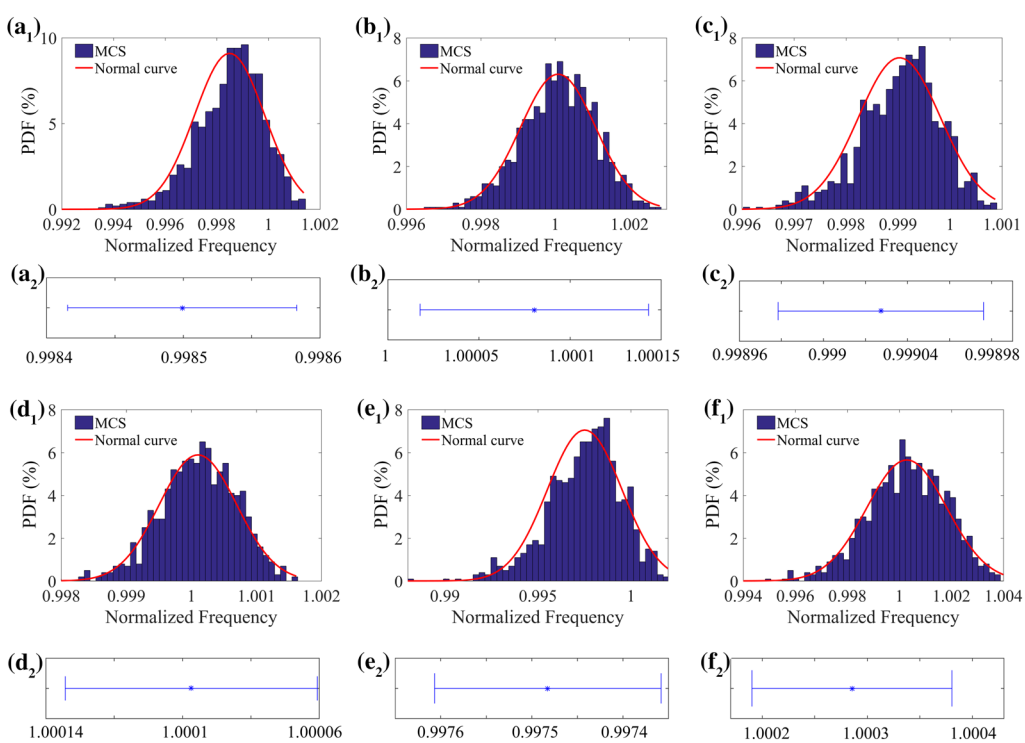

Figure 8 Probability density and the 95% confidence interval and mean of the first six frequencies for1000 random samples about mistuned restraint stiffness with $\sigma_k = 20\%$: **a** The first order; **b** the second order; **c** the third order; **d** the fourth order; **e** the fifth order; **f** the sixth order (subscript 1 represents the probability density, subscript 2 represents the 95% confidence interval and mean)

Table 5 A random mistuned restraint stiffness in the radial direction with the standard deviation $\sigma_k = 20\%$

No.	Stiffness	No.	Stiffness
1	9751711.30356738	9	10977787.5406236
2	12979395.2155709	10	12069386.0198357
3	12818068.979601	11	11453770.2667665
4	12834384.8268592	12	9393118.15042797
5	11342994.2672162	13	10587742.9341933
6	7585026.15462992	14	8425434.39248272
7	11434477.3026577	15	11776791.2635153
8	13260470.5783295	16	7705859.7860617

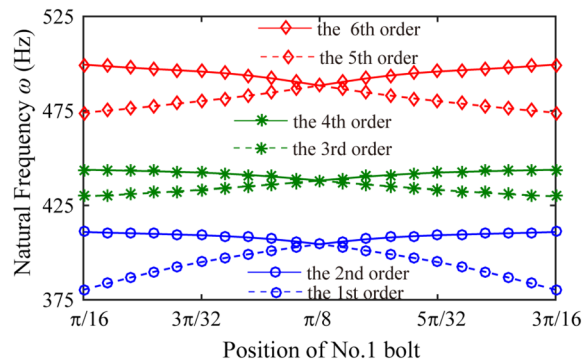

Figure 10 Effect of the position of only one mistuned bolt (No.1 bolt) on the first six natural frequency

of the first six frequencies are plotted in Figure 5 through the Monte Carlo simulation method by considering the standard deviation $\sigma_\theta = 10\%$. 1000 samples were calculated here. And a normal curve of $N(\overline{\omega}, S_\sigma^2)$ also is plotted to estimate the frequency distribution. As shown, it can be found that most of the 1st, 3rd and 5th order normalized frequencies are all lower than 1. And the most of the frequencies of the 2nd, 4th and 6th order are larger than 1. From Figure 5, it can be found the frequency distribution has a good agreement with the normal curve, which indicates that mode frequencies with random mistuned bolt distribution follow an approximately normal distribution under the standard deviation $\sigma_\theta = 10\%$. Moreover, a 95% confidence level is considered for reliability analysis. The means and confidence intervals of the first six frequencies with $\sigma_\theta = 10\%$ are also plotted in Figure 5.

Then, an example of a random mistuned bolt distribution is presented to help understand the mode characteristics of the cylindrical shell. The random mistuning pattern of bolt position is tabulated in Table 3. The first six frequencies and mode shapes are presented in Table 4 and are plotted in Figure 6, respectively. Comparing the frequencies in Tables 2 and 4, the obvious difference can be found, especially for the first, third, fifth and sixth order. And it can be also found that the same frequency break into two different frequencies. At the same time, compared with Case Ⅰ in Figure 3, the mode shapes in Figure 6 have significant changes when the bolt distribution varies from the tuned case. And the obvious changes in the shapes have been pointed out in the figures.

5.2 Effect of the Restraint Stiffness Random Mistuning

For bolt joints, the theoretical condition about the restraint stiffness of the bolted joints for the cylindrical shell is as the absolute same as each other. However, due to material property error of the bolts, installation error such as preload of the bolts or even the nonlinear characteristics of bolted joints under external excitations, the restraint stiffness of these bolts may have a difference with each other, what's more, the stiffness difference is indeterminate. The case that the restraint stiffness of the bolts is not equal to each other is defined as the restraint stiffness mistuning here. Therefore, this section aims to investigate the effect of random restraint stiffness

Table 6 The normalized frequencies of cylindrical shell with a random mistuned restraint stiffness sample with $\sigma_k = 20\%$

Order	1	2	3	4	5	6
Frequency	404.67	405.19	438.00	438.55	488.40	489.94

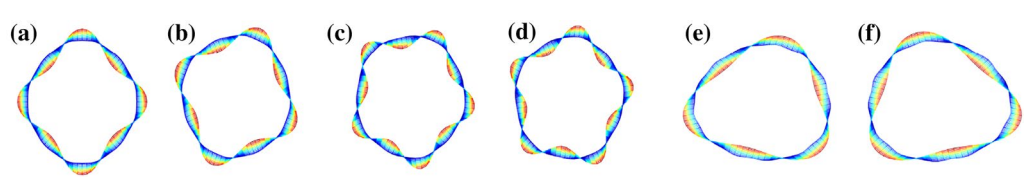

Figure 9 Mode shapes of the cylindrical shell with a random mistuned restraint stiffness sample with $\sigma_k = 20\%$: **a** The first order; **b** the second order; **c** the third order; **d** the forth order; **e** the fifth order; **f** the sixth order

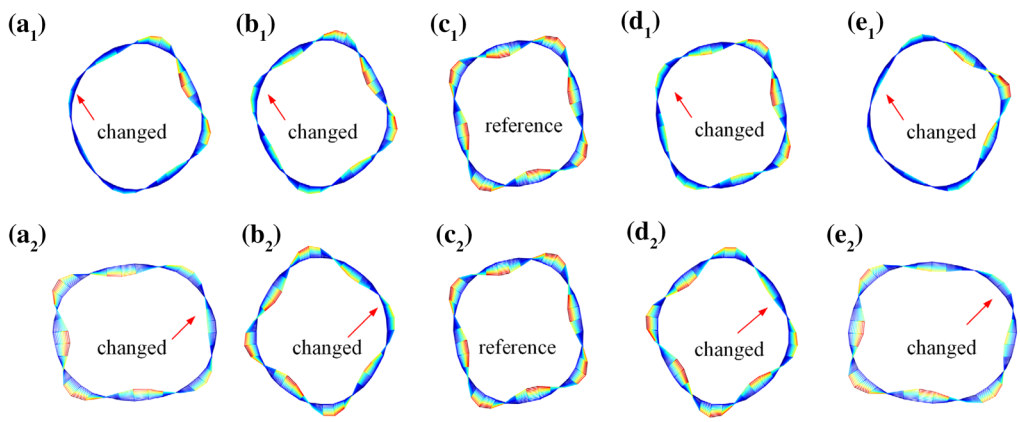

Figure 11 Mode shapes of cylindrical shell with different position of No. 1 bolt: **a** $\theta_1 = \pi/16$; **b** $\theta_1 = 3\pi/32$; **c** $\theta_1 = \pi/8$; **d** $\theta_1 = 5\pi/32$; **e** $\theta_1 = 3\pi/16$ (subscript 1 represents the first order mode, subscript 2 represents the second mode)

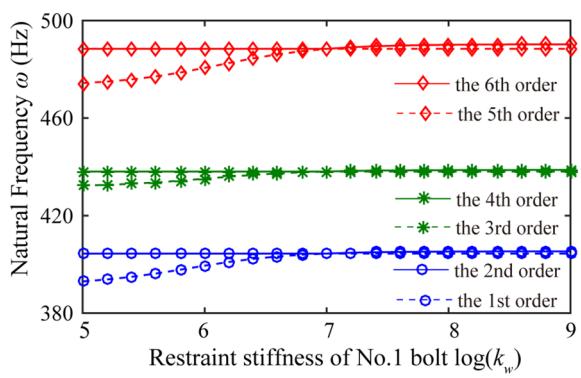

Figure 12 Effect of the restraint stiffness of only one mistuned bolt (No. 1 bolt) on the first six natural frequency

mistuning of the bolts on the mode characteristics of the cylindrical shell. In calculation, the MCS technique is employed. It is assumed the sample number is $N_S = 1000$. The radial restraint stiffness is selected to be the mistuned parameter here as an example and the radial restraint stiffness error follows a normal distribution law $N(0, \sigma_k^2)$. The restraint stiffness in the other directions is set to be a constant value.

Figure 7 plots the first six frequency means of the shell with the random radial restraint stiffness for the samples. The statistical results show, with the standard deviation $\sigma_k = 10\%$, the odd order frequency means of the mistuned system are smaller than the frequency of the tuned system, and the even order frequency means are larger than the frequency of the tuned system. However, all the normalized frequency means decreases obviously as the standard deviations of the mistuning error of the restraint stiffness increases. When the standard deviation $\sigma_k = 30\%$, the first six normalized frequency means are all lower than 1.

Figure 8 shows the distributed characteristics of the first six frequencies of the bolted joined cylindrical shell

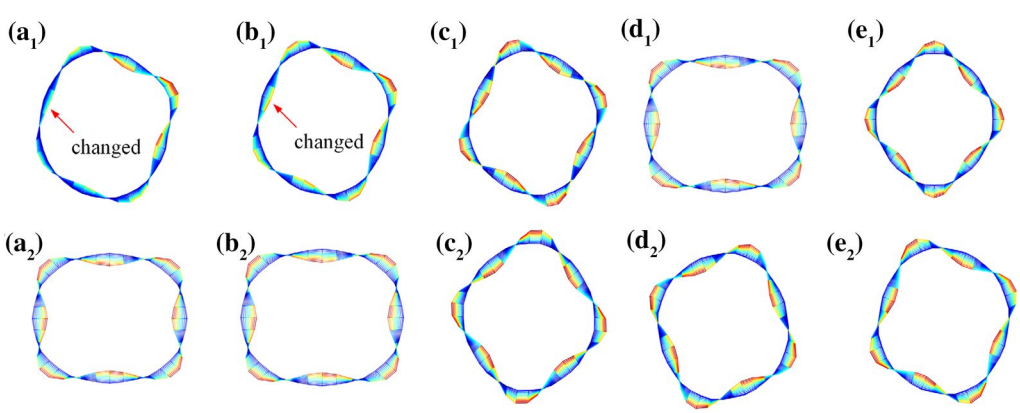

Figure 13 Mode shapes of cylindrical shell with restraint stiffness of No. 1 bolt: **a** $\log(k_w) = 5$; **b** $\log(k_w) = 6$; **c** $\log(k_w) = 7$; **d** $\log(k_w) = 8$; **e** $\log(k_w) = 9$ (subscript 1 represents the first order mode, subscript 2 represents the second mode)

by using MCS and considering $\sigma_k = 20\%$ of the restraint stiffness error for 1000 samples. The histogram for the probability density function (PDF) of the frequency. As demonstrated, the probability density function of the odd order frequency is an asymmetrical distribution pattern about the frequency means and the left frequency band $\left[\omega_{\min}/\omega_{\mathrm{t}}, \overline{\omega}\right]$ is wider than the right band $\left[\overline{\omega}, \omega_{\max}/\omega_{\mathrm{t}}\right]$. And the even order similarly follows a symmetrical distribution pattern about the frequency means. More, a red curve of a normal distribution $N(\overline{\omega}, S_{\sigma}^2)$ was to estimate the frequency distribution of the samples of mistuned systems. By comparing the frequency distribution and normal curve in the figures, the results show the frequency follows an approximately normal distribution. And a 95% confidence level is also considered for reliability analysis.

Then, an example of a random mistuned restraint stiffness is presented to better understand the cylindrical shell's vibration characteristics. The random mistuning pattern of restraint stiffness is tabulated in Table 5. The first six frequencies and mode shapes are listed in Table 6 and are plotted in Figure 9, respectively. Comparing the frequencies in Table 2 and Table 6, it is found the random mistuned stiffness bring the variation of the frequencies. Although the frequency variation in this example is small, it is obvious the same frequency break into two different frequencies. At the same time, compared with Case Ⅰ in Figure 3, the mode shapes in Figure 9 also have a slight change which is hardly intuitively found in the present case here, because the restraint stiffness are close to the tuned case, which will be further discussed in the following section.

5.3 Discussion

To explain the influence of the mistuned bolt position on free vibration of the cylindrical shell, a special case was presented. The position of the mistuned bolt (No. 1) is changed in the range from π/16 to 3π/16 and other bolts keep unchanged. As shown in Figure 10, it is easily found that the natural frequencies have obvious variations as the position of No. 1 bolt was changed. When θ_1 is π/8, the system is a tuned system, as introduced above, there is a pair of two same frequencies, such as the 1st and the 2nd order, and they have the similar shapes. However, as the θ_1 deviates from π/8, one of these two frequencies (the 1st order) obviously decreases, and the other slightly increases (the 2nd order). The variation of mode shapes of the first two order is shown in Figure 11, as shown, when $\theta_1 = \pi/8$, the same frequencies and the same mode shapes. However, as θ_1 is not equal to π/8, the mode shapes are changed and they are not the symmetrical shapes, which have been pointed in Figure 11. As the mistuning value increase, the difference of the mode shapes between the mistuned system and the tuned system gets larger. The results indicate the bolt position plays an important role in natural frequency and mode shape of the cylindrical shell. Moreover, the vibration characteristics of the cylindrical shell will be more complex with the mult-bolts mistuning or even random mistuning. These are why the frequency means are larger than 1 or less than 1 in Figure 4 and also the explanation of the frequency distribution of the samples in Figure 5. Therefore, it is necessary to study the vibration characteristics of cylindrical shell with the bolt distribution random mistuning case with different the standard deviation and it will help for design, fabrication, and installation.

In the same way, to explain the influence of the random stiffness mistuning on the mode characteristic of the cylindrical shell, a special case was presented. The restraint stiffness $\log(k_w)$ of the mistuned bolt (No. 1) is changed in the range from 5 to 9 and other bolts keep unchanged. As shown in Figure 12, it is easily found that the natural frequencies have obvious variations as the stiffness of No. 1 bolt was changed. When $\log(k_w) = 7$, the system is a tuned system, as introduced above, there is a pair of two same frequencies and mode shapes. However, as the $\log(k_w)$ deviates from 7, the same frequencies are changed to two different value. As the stiffness decreases, the frequency decrease obviously. However, as the stiffness increase, the variation of the frequency is not so obvious. That is to say when the stiffness is beside $\log(k_w) = 7$, the increment of frequency per stiffness get less as the stiffness increase. These can be used to explain the frequency means decrease as the standard deviation increase in Figure 7, and the wider distribution at the left hand of means in Figure 8. The variation of mode shapes of the first two modes is shown in Figure 13 to help understand the effect of restraint stiffness on the mode characteristics.

6 Conclusions

The dynamic model of a cylindrical shell with bolted joints was established. The artificial spring technology was used to simulation the linear restraint effects of the bolted joints. The natural frequency and mode shape were focused on to interpret the mode characteristics of cylindrical shell with non-uniform parameters of bolt joint, which was expressed as two mistuning forms, such as bolt distribution and restraint stiffness. The effects of random bolt distribution mistuning and random restraint stiffness mistuning on natural frequencies were studied by the Monte Carlo simulation and based on statistical theory. And discussions were made. The conclusions can be obtained as follows.

(1) The mistuning patterns, such as the bolt distribution mistuning and the bolt restraint stiffness mistuning, not only impact the natural frequency, but also the mode shape. When a random mistuning pattern occurs, the symmetry of the restraint condition of the cylindrical shell is broken, which causes the repeated frequencies and mode shapes split into two different frequencies and the mode shapes.
(2) Considering the random bolt distribution mistuning, the frequency means deviate from the tuned system as the standard deviation increase. In the present sample, the frequency follows an approximately normal distribution. Therefore, the reasonable and symmetrical distribution will help reduce the complexity of mode characteristics of the cylindrical shell.
(3) Considering the bolt restraint stiffness mistuning, in the present case, the frequency means of the mistuned samples decrease as the standard deviation of the mistuning error increases, and the frequency follows an approximately normal distribution. Moreover, the tightening torque, tightening sequence, and other factors, which mainly affect the restraint stiffness, should be further discussed in the following study to help reduce the complexity of dynamic characteristics of shell structures.

Acknowledgements
Not applicable.

Authors' Contributions
CL was in charge of the theory modelling and the whole structure of articles; QT wrote the manuscript; QT and HS assisted with simulation and analysis; BW make some significant advice. All authors read and approved the final manuscript.

Authors' Information
Qiansheng Tang, born in 1989, is currently a lecturer at *School of Engineering, Anhui Agricultural University, China*.
Houxin She, born in 1990, obtained the PhD degree from *School of Mechanical Engineering & Automation, Northeastern University, China*.
Chaofeng Li, born in 1980, PhD, is currently a professor at *School of Mechanical Engineering & Automation, Northeastern University, China*. His research interests include mechanical dynamics and control.
Bangchun Wen, born in 1930, is a professor at *School of Mechanical Engineering & Automation, Northeastern University, China*. His research interests include vibration utilization engineering.

Funding
Supported by Anhui Provincial Natural Science Foundation of China (Grant No. 2108085QE223), Universities Natural Science Research Project of Anhui Province of China (Grant No. KJ2021A0156), and National Natural Science Foundation of China (Grant Nos. 52075086, 52205078).

Data availability
All data and materials generated or analyzed during this study are included in this article. But the processed data required to reproduce these findings cannot be shared at this time due to legal or ethical reasons.

Competing Interests
The authors declare no competing financial interests.

Received: 10 February 2023 Revised: 10 February 2023 Accepted: 17 February 2023
Published online: 06 April 2023

References
[1] D Yadav, N Verma. Free vibration of composite circular cylindrical shells with random material properties. Part I: General theory. *Composite Structures*, 1998, 41: 331-338.
[2] D Yadav, N Verma. Free vibration of composite circular cylindrical shells with random material properties. Part II: Applications. *Composite Structures*, 2001, 51: 371-380.
[3] L Rodrigues, F M A Silva, P B Goncalves. Influence of initial geometric imperfections on the 1: 1: 1: 1 internal resonances and nonlinear vibrations of thin-walled cylindrical shells. *Thin-Walled Structures*, 2020, 151: 106730.
[4] L Rodrigues, F M A Silva, P B Gonçalves. Effect of geometric imperfections and circumferential symmetry on the internal resonances of cylindrical shells. *International Journal of Non-Linear Mechanics*, 2022, 139: 103875.
[5] A H Karimi, M Shadmani. Nonlinear vibration analysis of a beam subjected to a random axial force. *Archive of Applied Mechanics*, 2019, 89: 385-402.
[6] S Yang, Q Yang. Geometrically nonlinear random vibration responses of laminated plates subjected to acoustic excitation. *AIAA Journal*, 2018, 56: 2827-2839.
[7] T P Chang, H C Chang, M F Liu. A finite element analysis on random vibration of nonlinear shell structures. *Journal of Sound and Vibration*, 2006, 291: 240-257.
[8] L Dai, T J Yang, J T Du, et al. An exact series solution for the vibration analysis of cylindrical shells with arbitrary boundary conditions. *Applied Acoustics*, 2013, 74: 440-449.
[9] Z Y Qin, F L Chu, Z U Jean. Free vibrations of cylindrical shells with arbitrary boundary conditions: A comparison study. *International Journal of Mechanical Sciences*, 2017, 133: 91-99.
[10] H J Zhou, W Li, B Lv, et al. Free vibrations of cylindrical shells with elastic-support boundary conditions. *Applied Acoustics*, 2012, 73: 751-756.
[11] Y H Chen, G Y Jin, Z G Liu. Free vibration analysis of circular cylindrical shell with non-uniform elastic boundary constraints. *International Journal of Mechanical Sciences*, 2013, 74: 120-132.
[12] K Xie, M Chen, L Zhang, et al. Free and forced vibration analysis of non-uniformly supported cylindrical shells through wave based method. *International Journal of Mechanical Sciences*, 2017, 128: 512-526.
[13] C F Li, P Y Li, B F Zhong, et al. Geometrically nonlinear vibration of laminated composite cylindrical thin shells with non-continuous elastic boundary conditions. *Nonlinear Dynamics*, 2019, 95: 1903-1921.
[14] H Li, M W Zhu, Z Xu, et al. The influence on modal parameters of thin cylindrical shell under bolt looseness boundary. *Shock and Vibration*, 2016: 1-15.
[15] Z Y Qin, Q K Han, F L Chu. Bolt loosening at rotating joint interface and its influence on rotor dynamics. *Engineering Failure Analysis*, 2015, 59: 456-466.
[16] X Liao, J R Zhang, X Y Xu. Analytical model of bolted joint structure and its nonlinear dynamic characteristics in transient excitation. *Shock and Vibration*, 2016, 2016: 1-12.
[17] X Liao, J R Zhang, X Y Xu, et al. Dynamic response analysis in bolted joint structure with viscoelastic layer and experimental investigations. *Journal of Vibroengineering*, 2017, 19(3): 1585-1596.
[18] L B Zhu, A H Bouzid, J Hong. Analytical evaluation of elastic interaction in bolted flange joints. *International Journal of Pressure Vessels and Piping*, 2018, 165: 176-184.
[19] L B Zhu, A H Bouzid, J Hong, et al. Elastic interaction in bolted flange joints: An analytical model to predict and optimize bolt load. *Journal*

of Pressure Vessel Technology-Transactions of the ASME, 2018, 140(4): 041202-1-10.
[20] F Adel, O M Jamal. Vibration of nonlinear bolted lap-jointed beams using Timoshenko theory. *Archive of Applied Mechanics*, 2018, 88(6): 981-997.
[21] J Armand, L Salles, C W Schwingshackl, et al. On the effects of roughness on the nonlinear dynamics of a bolted joint: A multiscale analysis. *European Journal of Mechanics A-Solids*, 2018, 70: 44-57.
[22] H Li, HY Lv, H Sun, et al. Nonlinear vibrations of fiber-reinforced composite cylindrical shells with bolt loosening boundary conditions. *Journal of Sound and Vibration*, 2021, 496:115935
[23] C F Li, R H Qiao, Q S Tang, et al. Investigation on the vibration and interface state of a thin-walled cylindrical shell with bolted joints considering its bilinear stiffness. *Applied Acoustics*, 2021, 172: 107580.
[24] Q S Tang, C F Li, H X She, et al. Vibration analysis of bolted joined cylindrical-cylindrical shell structure under general connection condition. *Applied Acoustics*, 2018, 140: 236-247.
[25] H Li, Z Y Zou, Y Y Yan, et al. Free and forced vibrations of composite cylindrical–cylindrical shells with partial bolt loosening connections: Theoretical and experimental investigation. *Thin-Walled Structures*, 2022, 179: 109671.
[26] T R Yang, H Ma, Z Y Qin, et al. Coupling vibration characteristics of the shaft-disk-drum rotor system with bolted joints. *Mechanical Systems and Signal Processing*, 2022, 169: 108747.
[27] A Pirdayr, M Mohammadi, M J Kazemzadeh-Parsi, et al. Self-loosening effects on vibration characteristics of plates with bolted joints: An experimental and finite element analysis. *Measurement*, 2021, 185: 109922.
[28] D Du, W Sun, H Ma, et al. Vibration characteristics analysis for rotating bolted joined cylindrical shells considering the discontinuous variable-stiffness connection. *Thin-Walled Structures*, 2022, 177: 109422.
[29] F Wang, J Li, Y Q Liu, et al. The investigation of vibration characteristics on the bolted disk-drum joints structure. *Advances in Mechanical Engineering*, 2019, 11(3): 1-9
[30] R Lacayo, L Pesaresi, J Gross, et al. Nonlinear modeling of structures with bolted joints: A comparison of two approaches based on a time-domain and frequency-domain solver. *Mechanical Systems and Signal Processing*, 2019, 114: 413-438.
[31] M Beadoin, K Behdinan. Analytical lump model for the nonlinear dynamic response of bolted flanges in aero-engine casings. *Mechanical Systems and Signal Processing*, 2019, 115: 14-28.
[32] H X She, C F Li, G B Zhang, et al. Statistical investigation on the coupling mode characteristics of a blade-disk-shaft unit. *Mechanics Based Design of Structures and Machines,* 2021: 1-18.